Electrical Engineering in Japan, Vol. 167, No. 4, 2009
Translated from Denki Gakkai Ronbunshi, Vol. 127-D, No. 7, July 2007, pp. 685–692

Operating Principles of pin Diodes

IKUNORI TAKATA
Mitsubishi Electric Corp., Japan

SUMMARY

Analytical models of the pin diode in a small-current operation are not known yet. This article presents a simple analytical model of the pin diode operation with its confirmation by a numerical simulation. At the onset, carrier recombinations are not included for the sake of simplicity. The exact $J_F - V_F$ characteristic [$J_F \propto \exp(V_F/kT)$] could have been induced only by accounting for the Boltzmann distribution of each carrier across the junctions and the diffusion current of each minority carrier in a p-anode or n-cathode. Based on this new model, the modifications of hole–electron densities product ($n_e n_h$) across junctions, a rough estimation of the large operational current, its carrier distributions, and the effect of carrier recombination on the carrier distribution are plainly estimated and are also compared with the simulation results. © 2009 Wiley Periodicals, Inc. Electr Eng Jpn, 167(4): 47–56, 2009; Published online in Wiley InterScience (www.interscience.wiley.com). DOI 10.1002/eej.20844

Key words: pin diode; operation model; hole–electron densities product; Boltzmann distribution; large-current operation; carrier recombination.

1. Introduction

Equation (1) is known as the small-current operation equation for a pn diode [1]. Here, the diffusion lengths (L_h, L_e) are dependent on the lifetime (τ) ($L = \sqrt{D\tau}$). However, in the simplest diode, a state in which carrier recombination ($\tau = \infty$) can be considered. As a result, Eq. (1) is not appropriate as a basic equation for diode operation. Because Eq. (1) does not include the cathode n region concentration as a parameter, it is not applicable to a pin diode. (D_h and D_e are the diffusion coefficients; N_D and N_A represent the concentration of impurities in the n, p region).

$$J = J_h + J_e = q n_i^2 \left(\frac{D_h}{L_h N_D} + \frac{D_e}{L_e N_A} \right) \exp\left(\frac{qV}{kT} \right) \quad (1)$$

Several models for the large-current operation in a pin diode have been proposed, but almost no simple models of small-current operation are known [2]. There are very few specific analytical examples [3]. In this paper the author provides a basic analytical equation for when there is no recombination in the most basic structure. Then the approximate current values for large-current operation and the internal carrier distribution are clearly explained based on this. The author confirms the validity of this work through device simulations.

2. The Simplest pin Diode

The pin (pn^-n) diode considered here is a simplification where impurities of the p region, $i(n^-)$ region, and n region are constant (N_p, N_I, N_n), and the thickness (t_p, t_n) of the p region and n region is 10 μm or less. The carrier recombination mechanism is not included ($\tau = \infty$).

Figures 1 and 2 show typical examples of the distribution of the free electron density (n_e) and the hole electron density (n_h) in the on state. The densities (n_e, n_h) for the free

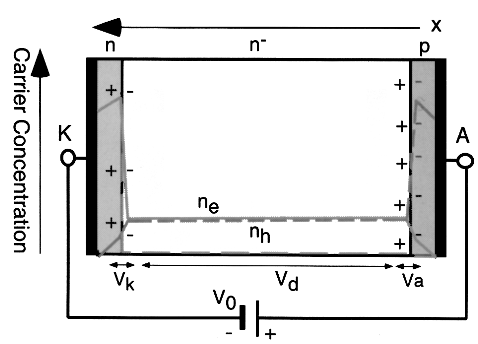

Fig. 1. Carrier distribution and voltage sharing of pin diode.

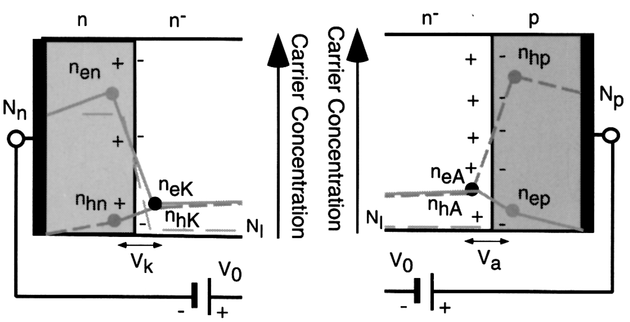

Fig. 2. (a) Cathode side distribution. (b) Anode side distribution.

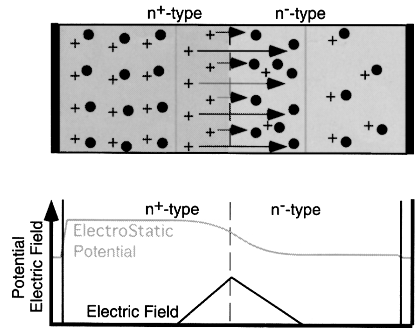

Fig. 3. Electric field and electrostatic potential ($V_{n^-n^+}$) at n^+n^- junction.

electrons and hole electrons at the boundaries at the two connections are (n_{en}, n_{hn}) in the n region, (n_{eK}, n_{hK}) on the cathode side of the i region, (n_{eA}, n_{hA}) on the anode side of the i region, and (n_{ep}, n_{hp}) on the p side. The orientation of the coordinate system (x axis) is along the flow of current.

3. Analysis of the Small-Current Operation

A difference in density in the carrier (free electrons and holes) occurs based on the concentration of impurities in the n^+n^- connection and the n^-p connection in a pin diode. For this reason, a carrier (free electrons) in the n region, for instance, where the concentration is higher diffuses to the n^- region where the concentration is lower. Positive ions remain after the free electrons have moved (Fig. 3). Then, an electric field occurs in the direction of the shift of free electrons between these + ions and the free electrons after their move. When a voltage is not applied externally, the region where this positive or negative electric charge is found expands until the speed of movement of the "free electrons" due to the generated electric field is equal to the speed of diffusion due to the difference in concentration.

As a result, in a balanced state, the state does not change at all even if the carrier in both regions is replaced.

In this state, both regions are in thermal equilibrium. A difference in only the integral value of the electric field based on the difference in density of the carrier present in the coupling occurs between the majority of the n^+ region separated by the coupling and the static potential (below abbreviated as potential) in the majority of the n^- region. A potential difference then occurs even in the connection boundary with the electrodes for the n^+ region and the n^- region. If the electrode metals are the same, then the (contact) potential difference for both connections is different only by the potential difference occurring at the n^+– n^- boundary. As a result, ultimately the potential on the electrode surfaces on both sides is equal. The potential difference created by the difference in the concentration of impurities (or the difference in semiconductor materials) in the semiconductor does not appear outside, and so is referred to as "built-in potential." Below, the built-in potential at the nn^- connection and the n^-p connection will be represented as V_{n^-n} and V_{pn^-}.

As can be seen in Fig. 3, the internal potential in the n^- region is lower than the internal potential in the n^+ region ($V^{+}_{n^-n} < 0$). Moreover, as can be seen in Fig. 4, the internal potential in the p region at the np junction is lower than the potential in the n region ($V_{pn} < 0$). For the np junction, the electric field occurs between the positive ions and the negative ions in each region n and p. Ultimately, it is clear that the internal potential is greater in a region with a higher concentration of free electrons.

If the forward voltage (V_0) is added to the pin diode from outside, then the electric potential is distributed to the nn^- junction (V_k), the n^- region (V_d), and the n^-p junction (V_a), as can be seen in Fig. 1 ($V_0 = V_k + V_d + V_a$). V_k and V_a boost the original built-in potential (V_{n^-n} and V_{pn^-}). The potential difference at the nn^- junction is $V_{n^-n} + V_k$, and at the n^-p junction is $V_{pn^-} + V_{n^-n}$ and V_{pn^-} are negative values, and so the absolute values for either are smaller.

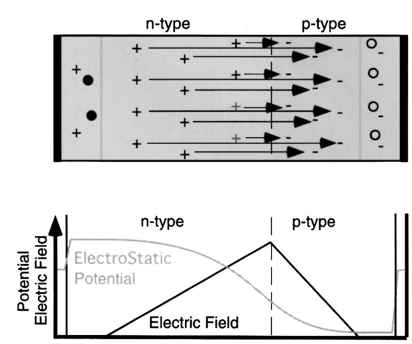

Fig. 4. Electric field and electrostatic potential (V_{pn}) at np junction.

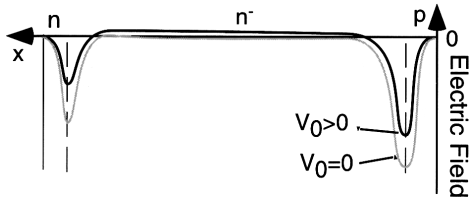

Fig. 5. Electric field distributions on forward operation (x-axis is oriented to the currents as shown in Fig. 1).

If a forward voltage (V_0) is applied, then the balanced state of movement due to the electric field present between the junctions and of movement due to the difference in the concentration changes. At the n^-p junction, the holes increase in number in the n^- region after shifting from the p region ($n_i^2/N_I \rightarrow n_{hA}$), and a new balanced state is reached where the shift due to the difference in the concentration is dominant [Fig. 2(b)]. The density of free electrons and holes in the n^- region is a value that satisfies the charge neutral condition ($n_{eA} \approx n_{hA} + N_I$). The shift due to the difference in the concentration is also dominant for the free electrons, and the density of free electrons on the left edge of the p region increases ($n_i^2/N_p \rightarrow n_{ep}$). The density of free electrons is the original value for the p region ($n_i^2/N_p \approx 0$) at the junction for the anode electrode,* and as a result, current proportional to the density slope (n_{ep}/t_p) where the density difference (n_{ep}) is divided by the width (t_p) of the p region flows, which is to say that the diffusion current (J_e) is generated [Eq. (2)]. Even for the nn^- junction, if the holes are considered instead of the free electrons and the shift direction is reversed, then the state is equivalent [Fig. 2(a)]. In the n region, the diffusion current for the hole electrons flows [Eq. (3)].†

In a state without carrier recombination, the electron current (J_e) and the hole current (J_h) are each constant in all regions in the diode:

$$J_e = qD_{ep}\frac{dn_e}{dx} = \mu_{ep}kT\frac{n_{ep}}{t_p} \tag{2}$$

$$J_h = -qD_{hn}\frac{dn_h}{dx} = -\mu_{hn}kT\frac{-n_{hn}}{t_n} \tag{3}$$

On the other hand, if an arbitrary ideal particle is present in the two regions in contact, the density of ideal particles in region a and region b are N_a and N_b, and the energy in region a based on region b sensed by the ideal particles is ΔE_{ab}, then the Boltzmann distribution shown in Eq. (4) for a state based on thermal equilibrium can be expected to hold‡:

$$\exp\left(\frac{-\Delta E_{ab}}{kT}\right) = \frac{N_a}{N_b} \tag{4}$$

For instance, when an external potential (V_0) is not applied, the ratio $[N_p/(n_i^2/N_I)]$ of the positive electron density in the n^-p junction and the potential difference (V_{pn^-}) is represented by the relationship in Eq. (5), and the ratio (N_n/N_I) of the free electron density in the nn^- junction and the potential difference (V_{n^-n}) is represented by the relationship in Eq. (6):

$$\exp\left(\frac{-qV_{pn^-}}{kT}\right) = \frac{N_p}{n_i{}^2/N_I} \tag{5}$$

$$\exp\left(\frac{qV_{n^-n}}{kT}\right) = \frac{N_I}{N_n} \tag{6}$$

Moreover, the relationship in Eq. (7) exists between the potential difference ($V_{pn^-} + V_a$) across the n^-p junction shown in Fig. 2(b), the ratio of the hole electron density (n_{hA}/n_{hp}), and the ratio of the free electron density (n_{eA}/n_{ep}). In the same fashion, the relationship in Eq. (8) exists between the potential difference ($V_{n^-n} + V_k$) across the nn^- junction, the ratio (n_{hK}/n_{hn}) of the electron hole density, and the ratio of the free electron density (n_{eK}/n_{en}).

$$\exp\left[\frac{-q(V_{pn^-} + V_a)}{kT}\right] = \frac{n_{eA}}{n_{ep}} = \frac{n_{hp}}{n_{hA}} \tag{7}$$

$$\exp\left[\frac{-q(V_{n^-n} + V_k)}{kT}\right] = \frac{n_{hK}}{n_{hn}} = \frac{n_{en}}{n_{eK}} \tag{8}$$

$\exp\,[q(V_a + V_k)/kT]$ can be altered into Eq. (9), but Eqs. (10) and (11) can also be combined and represented as Eq. (12). Combining Eqs. (9) and (12), and then taking the square root results in Eq. (13):

$$\exp\left[\frac{q(V_a+V_k)}{kT}\right] = \frac{\exp\left[\frac{q(V_{pn^-}+V_a)}{kT}\right]\exp\left(\frac{q(V_{n^-n}+V_k)}{kT}\right)}{\exp\left(\frac{qV_{pn^-}}{kT}\right)\exp\left(\frac{qV_{n^-n}}{kT}\right)} = \frac{n_{ep}}{n_{eA}}\frac{n_{hn}}{n_{hK}}\frac{N_p}{n_i{}^2/N_I}\frac{N_n}{N_I} = \frac{n_{ep}n_{hn}}{n_i{}^2}\frac{N_pN_n}{n_{eA}n_{hK}} \tag{9}$$

$$\exp\left(\frac{qV_a}{kT}\right) = \frac{\exp\left(\frac{-qV_{pn^-}}{kT}\right)}{\exp\left[\frac{-q(V_{pn^-}+V_a)}{kT}\right]} = \frac{\frac{N_p}{n_i{}^2/N_I}}{\frac{n_{hp}}{n_{hA}}} \approx \frac{n_{hA}}{n_i{}^2/N_I} \tag{10}$$

$$\exp\left(\frac{qV_k}{kT}\right) = \frac{\exp\left(\frac{-qV_{n^-n}}{kT}\right)}{\exp\left[\frac{-q(V_{n^-n}+V_k)}{kT}\right]} = \frac{\frac{N_n}{N_I}}{\frac{n_{en}}{n_{eK}}} \approx \frac{n_{eK}}{N_I} \tag{11}$$

$$\exp\left[\frac{q(V_a+V_k)}{kT}\right] \approx \frac{n_{hA}n_{eK}}{n_i{}^2} \approx \frac{(n_{eA}-N_I)(n_{hK}+N_I)}{n_i{}^2} \approx \frac{n_{eA}n_{hK}}{n_i{}^2} \tag{12}$$

$$\exp\left[\frac{q(V_a+V_k)}{kT}\right] \approx \frac{\sqrt{n_{ep}n_{hn}N_pN_n}}{n_i{}^2} \tag{13}$$

*Simulator definition of an ohmic junction.

†The relational equation [$D = (kT/q)\mu$] by Einstein is used to change the formula. Also, the x axis is in the direction of the current.

‡In Section 4, the validity is argued and confirmed through simulations.

The following relational equations are used for these calculations [refer to Figs. 2(a) and 2(b)]. The equal sign in Eqs. (14) and (16) refers to the charge neutral condition in the p region and n region. The charge neutral condition almost holds in the n^- region as well [Eqs. (15) and (17)].

$$n_{hp} = N_p + n_{ep} \approx N_p \tag{14}$$

$$n_{hA} \approx n_{eA} - N_I \tag{15}$$

$$n_{en} = N_n + n_{hn} \approx N_n \tag{16}$$

$$n_{eK} \approx n_{hK} + N_I \tag{17}$$

If n_{ep} and n_{hn} resulting from Eqs. (2) and (3) are substituted into Eq. (13), then Eq. (18) results:

$$\exp\left[\frac{q(V_a+V_k)}{kT}\right] \approx \sqrt{\frac{J_e t_p}{\mu_e kT}}\sqrt{\frac{J_h t_n}{\mu_h kT}}\frac{\sqrt{N_p N_n}}{n_i^2} \tag{18}$$

If we take the density of the free electrons and the holes in the n^- region as equivalent ($n_e \approx n_h$), then the ratio (J_e/J_h) of the current density of the two can be approximated by the ratio (μ_{eI}/μ_{hI}) of the mobility [Eq. (19)]. If the ratio (μ_{ep}/μ_{hn}) of the mobility (μ_{ep}) of the free electrons in the p region and the mobility (μ_{hn}) of the hole electrons in the n region is approximately equal to the ratio (μ_{eI}/μ_{hI}), then Eq. (20) showing the current density (J_e) for the holes results. Equation (21), which combines this with the electron current density (J_e), represents the total current (J). As a result, a relationship in which the total current (J) is proportional to the exponential function for the sum ($V_a + V_k$) of the external potentials that the n^-p junction and the nn^- junction bear results.

$$J_e \approx \left(\frac{\mu_{eI}}{\mu_{hI}}\right) J_h \tag{19}$$

$$J_h \approx \frac{kTn_i^2\mu_{hn}}{\sqrt{N_p N_n t_p t_n}}\exp\left[\frac{q(V_a+V_k)}{kT}\right] \tag{20}$$

$$J = J_h + J_e \approx \frac{kTn_i^2(\mu_{hn}+\mu_{ep})}{\sqrt{N_p N_n t_p t_n}}\exp\left[\frac{q(V_a+V_k)}{kT}\right] \tag{21}$$

Equation (21) can be derived by the following simplifications.

(1) The net charge in the i region is almost zero ($n_e \approx n_h + N_I$).

(2) There is no recombination between the holes and the free electrons (the electron current and the hole electron current are constant in all regions).

(3) The approximation $J_e/J_h \approx \mu_{eI}/\mu_{hI}$ can be used, and the dependence on the impurity concentration in the mobility (μ) is ignored ($\mu_{ep}/\mu_{hn} \approx \mu_{eI}/\mu_{hI}$).

(4) The increase in the majority carriers in the n region and the p region is ignored ($n_{en} \approx N_n$, $n_{hp} \approx N_p$).

Because the voltage drop (V_d) in the i region can be ignored in the small-current operation, $V_a + V_k = V_0 - V_d \approx V_0$, and the total current (J) can be represented using an exponential function for the forward voltage (V_0), as shown in Eq. (22):

$$J \propto \exp\left(\frac{qV_0}{kT}\right) \tag{22}$$

Moreover, if Eq. (21) is modified using the Einstein relational equation [$D = (kT/q)\mu$], then Eq. (23), which resembles Eq. (1) that represents the small-current operation in the pn diode, results. The thickness (t_p, t_n) of the p or n region corresponds to the diffusion length (L_e, L_h) in Eq. (1). For instance, in an extreme case such as $N_p = N_n = N_D = N_A$ where $t_p = t_n = L_e = L_h$, Eqs. (23) and (1) match.

$$J = J_h + J_e \approx qn_i^2\frac{(D_{hn}+D_{ep})}{\sqrt{N_p N_n t_p t_n}}\exp\left[\frac{q(V_a+V_k)}{kT}\right] \tag{23}$$

(D: diffusion coefficient; N_n, N_p: concentration of impurities in the n and p regions).

4. Validity of the Boltzmann Distribution Approximation in the Small-Current Operation

In the calculations in the preceding section, we assumed that the carrier follows the Boltzmann distribution in Eq. (4) in a narrow region enclosing a junction (even in a state in which current was flowing). In this section, a procedure for calculations in a simulator is presumed. In the simplest drift-diffusion transport model in a device simulator, the following five equations are fundamental [4]. In the calculations, the Boltzmann distribution is clearly not used in the form found in Eq. (4).

$$\nabla(\epsilon \bullet \nabla\psi) = -q(n_h - n_e + N_D - N_A) \tag{24}$$

$$-\nabla \bullet J_h = qR + q\frac{\partial n_h}{\partial t} \tag{25}$$

$$\nabla \bullet J_e = qR + q\frac{\partial n_e}{\partial t} \tag{26}$$

$$J_h = -qD_h\nabla n_h - q\mu_h n_h \nabla\psi \tag{27}$$

$$J_e = qD_e\nabla n_e - q\mu_e n_e \nabla\psi \tag{28}$$

ψ: electrostatic potential; q: elementary charge (1.6×10^{-19} C); J_h, J_e: current density vector; R: speed of free electron and hole electron recombination (function of n_h and n_e); D_h, D_e: diffusion coefficients; μ_h, μ_e: drift mobility; $\bullet$: vector product. Equations (25) and (26) represent the carrier continuity. The "drift-diffusion transport model" is represented in Eqs. (27) and (28). The first element on the right of these equations is the diffusion current component, and the second element is the drift current component. (The subscripts h and e represent the hole and free electron components.)

However, in Eqs. (27) and (28) in the transport model, if the current density (J_h, J_e) is assumed to be zero, then the Boltzmann distribution [Eq. (4)] appears. For instance, if $J_h = 0$ is assumed in Eq. (27), then Eq. (29) results. If the Einstein relational equation [$D_h = (kT/q)\mu_h$] is applied to this,* and only the changes in the x direction are simplified, then partial integration can be performed, and the hole electron density (n_h) can be derived as an exponential function of the static potential (ψ) [Eq. (31)]. In the same fashion, Eq. (32) can be obtained for the free electron density (n_e) (C is the integration constant). In other words, in the "drift-diffusion transport model," in the state in which the net current density is zero ($J = 0$), the Einstein relational equation and the Boltzmann distribution have the same meaning.

$$\frac{1}{n_h}\frac{dn_h}{dx} = -\frac{\mu_h}{D_h}\frac{d\psi}{dx} \tag{29}$$

$$\frac{1}{n_h}\frac{dn_h}{dx} = -\frac{q}{kT}\frac{d\psi}{dx} \tag{30}$$

$$\int\frac{dn_h}{n_h} = -\frac{q}{kT}\int d\psi$$

$$\ln n_h = -\frac{q}{kT}\psi + C$$

$$n_h = C\exp\left(\frac{-q\psi}{kT}\right) \tag{31}$$

$$n_e = C\exp\left(\frac{q\psi}{kT}\right) \tag{32}$$

However, Eq. (30) can be interpreted as Eq. (33). This equation shows that the rate of spatial change (left side) of the thermal kinetic energy (kT) due to the diffusion movement per carrier particle and the rate of spatial change (right side) for the Coulomb energy ($q\psi$) due to drift movement are balanced. This state is natural when the magnitude of the movement speed due to both movements in Eq. (29) is equal in opposite directions. The Einstein relational equation is legitimate for an explanation based on the Boltzmann transport equations found in Ref. 5, but based on the rough explanation above, if $J = 0$, then the Boltzmann distribution can be interpreted as also holding.

$$\frac{1}{n_h}\frac{d(kTn_h)}{dx} = -\frac{d(q\psi)}{dx} \tag{33}$$

Even when the balance between the diffusion current and the drift current collapses and a net current equal to the difference between the two is flowing, if the rate of the net current is small, then both the Einstein relational equation and the Boltzmann distribution can be expected to be valid approximately.†

*In the device simulator, the mobility (μ) can be set arbitrarily, but this is not the case for the diffusion coefficient (D). As a result, the Einstein relational equation should be used.

Table 1. Maximum drift currents versus total currents at anode

	$J_{e.drift}$	$J_{h.drift}$
$J_{drift}(max)$	-35.7 kA/cm^2	63.3 kA/cm^2
$J_{e.net}$, $J_{h.net}$	-234 A/cm^2	-141 A/cm^2
$J_{drift}(max)/J_{net}$	x153	x(−446)

Table 1 provides a comparison of the current density (J_h, J_e) for the holes and free electrons obtained in the device simulator and the drift current component ($J_{h.drift}$, $J_{e.drift}$) near the anode junction. The percentage of the maximum value [J_{drift}(max)] in the drift current with respect to the net current density (J_e or J_h) is approximately 150 to 400 times greater, including when near the cathode junction. As a result, in an operating state at $V_{AK} = 1$ V or $J_A \approx 400$ A/cm^2 for a 100-µm pin diode, an approximation in which "the net current density (J_h, J_e) is effectively zero" is deemed allowable.

The diode configuration employed in the simulator has a uniform impurity density, and does not include carrier recombination mechanisms ($N_p = N_n = 10^{18}$ cm^{-3}; $N_I = 10^{14}$ cm^{-3}; $t_p = t_n = 10$ µm, $t_I = 100$ µm).

5. Changes in the $n_e n_h$ Product in the Regions at Junctions

The relationship in which the product $n_e n_h$ does not change at the boundary of the n^-p junction and the nn^- junction shown in Eqs. (34) and (35) can be derived directly from Eqs. (7) and (8), respectively.

$$n_{hA}n_{eA} = n_{hp}n_{ep} \tag{34}$$

$$n_{hK}n_{eK} = n_{hn}n_{en} \tag{35}$$

However, in a device with a high concentration of impurities in the p or n region, these relationships change a little due to the occurrence of band gap narrowing. Band gap narrowing is a simulation method that narrows the band gap (E_g) to reproduce in an equal fashion the phenomenon in which the state density of the valence bands and the con-

†Reference 6 explains that "although the Einstein relational equation holds when the Boltzmann distribution approximation in a state of thermal equilibrium is allowed, in practice the absolute values of the diffusion component and the drift component are large, and the two virtually cancel each other out, with only a small difference providing the current. As a result, the Einstein relational equation is often extended to non-equilibrium states." Moreover, Ref. 7 states that the Boltzmann distribution is valid in the pn junctions where the carrier density on one side is low.

duction bands in a semiconductor region with a high concentration of impurities [4]. As can be seen in Fig. 6, when band gap narrowing occurs, Eq. (4) is used for the holes and free electrons at the pn^- boundary and the n^-n boundary, and using the relationship [Eqs. (36) through (41)] corresponding to Eqs. (5) through (8), Eq. (42) can be derived. Equation (42) is different from Eq. (18) only in the exponent element on the right side. As a result, Eq. (43) can be derived based on changes to Eqs. (18) through (20). It is clear that the on operating current (J) increases only by the quantity ΔE_{gp} ($\equiv A + B$) and ΔE_{gn} ($\equiv C + D$). Only the sum of A and B or C and D exerts an influence, and these ratios are unrelated.

$$\exp\left[\frac{qV_{n^-n} - C}{kT}\right] = \frac{N_I}{N_n} \tag{36}$$

$$\exp\left[\frac{-q(V_{n^-n} + V_k) - D}{kT}\right] = \frac{n_{hK}}{n_{hn}} \tag{37}$$

$$\exp\left[\frac{q(V_{n^-n} + V_k) - C}{kT}\right] = \frac{n_{eK}}{n_{en}} \tag{38}$$

$$\exp\left[\frac{-qV_{pn^-} + B}{kT}\right] = \frac{N_p}{n_i^2/N_I} \tag{39}$$

$$\exp\left[\frac{-q(V_{pn^-} + V_a) + B}{kT}\right] = \frac{n_{hp}}{n_{hA}} \tag{40}$$

$$\exp\left[\frac{q(V_{pn^-} + V_a) + A}{kT}\right] = \frac{n_{ep}}{n_{eA}} \tag{41}$$

$$\exp\left[\frac{q(V_a + V_k)}{kT}\right] \approx \sqrt{\frac{J_e t_p}{\mu_e kT}}\sqrt{\frac{J_h t_n}{\mu_h kT}}\frac{\sqrt{N_p N_n}}{n_i^2}\exp\left(\frac{-(A+B+C+D)}{kT}\right) \tag{42}$$

$$J = J_h + J_e \approx \frac{kTn_i^2(\mu_h+\mu_e)}{\sqrt{N_p N_n t_p t_n}}\exp\left[\frac{q(V_a+V_k)+\Delta E_{gp}+\Delta E_{gn}}{kT}\right] \tag{43}$$

For the product $n_h n_e$ for the regions with opposing boundaries, Eqs. (44) and (45) can be derived from Eqs. (36) through (38), and a relationship between the band gap narrowing (ΔE_{gp}, ΔE_{gn}) and the temperature (T) exists.* When evaluating the carrier distribution in a bipolar device, these two equations are essential. These two equations plus Eqs. (34) and (35) represent one form of the law of mass action.

$$\frac{n_{hA} n_{eA}}{n_{hp} n_{ep}} = \exp\left(\frac{-\Delta E_{gp}}{kT}\right) \tag{44}$$

$$\frac{n_{hK} n_{eK}}{n_{hn} n_{en}} = \exp\left(\frac{-\Delta E_{gn}}{kT}\right) \tag{45}$$

*In the Slotboom model in Synopsis Inc.'s dessis, ΔE_g is 29 meV at 1×10^{18} cm^{-3}, 60.5 meV at 1×10^{19} cm^{-3}, 92 meV at 1×10^{20} cm^{-3}.

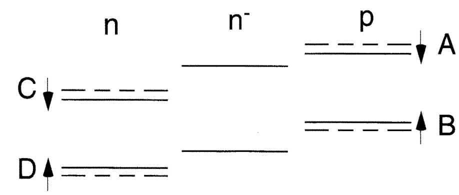

Fig. 6. Band gap narrowing.

Using the results of simulations for a t_{n^-} = 100 μm pin diode at V_{AK} = 1 V, Figs. 7(a) and 7(b) compare the difference in the carrier distribution (n_e, n_h, $n_e n_h$) based on whether or not band gap narrowing is present.

In Fig. 8, the $J_F - V_F$ characteristics are compared. In order to have Eq. (21), where $V_a + V_b = V_0$, match the line without band gap narrowing, $\mu_h + \mu_e$ was compared with 526 cm^2/Vs. This 526 cm^2/Vs is a value approximately 1.4 times greater than the mobility in the n region and p region shown by the simulator. The analytical equation in Eq. (21) is judged as approximating the simulation results well.

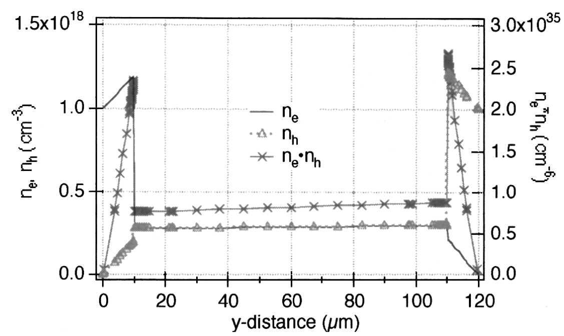

(a) with Band Gap Narrowing

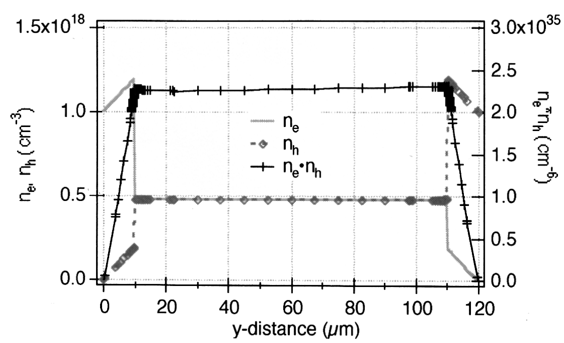

(b) without Band Gap Narrowing

Fig. 7. Effect of band gap narrowing on carrier distributions (V_{AK} = 1 V).

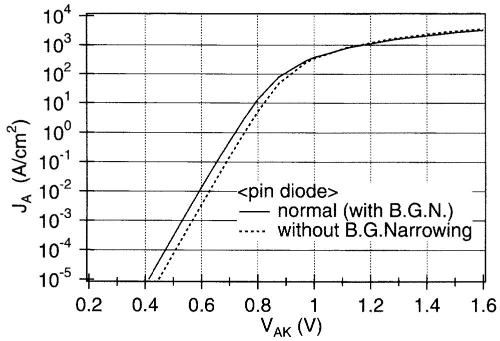

Fig. 8. Effect of band gap narrowing on $J_F - V_F$ characteristics ($V_{AK} = 1$ V).

6. Simulation Results for Medium- and Large-Current Operation

When the concentration of impurities in the *n* and *p* regions is the same, the carrier density (n_e, n_h) in the *i* region shown in the simulator is virtually constant in low-current operation. However, in (medium-current) operation where V_d can be ignored, an (almost) straight line sloping slightly toward the *n* side results (for instance, refer to Fig. 7 and the results of $V_F = 1$ V).

The reason for this is that the difference between the two narrows as the carrier mobility for the free electrons and the holes ($\propto$ diffusion coefficient) falls in the region with a high concentration of impurities. In other words, when "there is no recombination," the current density (J_e, J_h) of the free electrons and holes is constant throughout the *p*, *i*, and *n* regions. However, the ratio ($\mu_{ep}/\mu_{hn} = D_{ep}/D_{hn}$) of the mobility of free electrons in the *p* region and of the holes in the *n* region is smaller than the ratio (μ_{el}/μ_{hl}) of the mobility in the *i* region. As a result, in order for the drift current and the diffusion current for the holes and the free electrons at the junctions on both sides to continue, a configuration in which the free electron current in the *i* region is lower, and the hole current is higher must be used. This allows for adding diffusion from the anode to the cathode as a result of the biased carrier distribution.

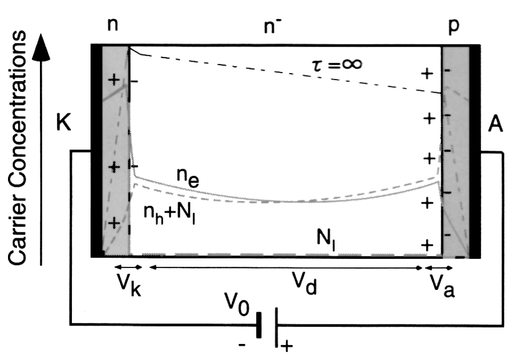

Fig. 9. Carrier distributions at large-current operation or high recombination rate.

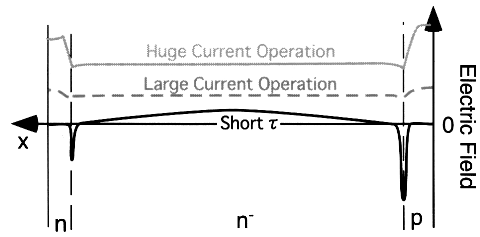

Fig. 10. Electric field distributions at large-current operation or high recombination rate.

However, when the carrier density (n_e, n_h) in large-current operation (in a pin diode with a symmetrical structure as found here) is in a state in which the concentration (N_l) of impurities in the n^- region is exceeded by several orders of magnitude, the slope leans toward the *p* anode side (dotted line in Fig. 9). This is because the slope ($\Delta n_h/t_n$) of the hole density in the *n* region must be greater than the slope ($\Delta n_e/t_p$) of the electron density in the *p* region, because the diffusion coefficient (D_{hn}) for the holes in the *n* region is smaller than that of the free electrons (D_{ep}) in the *p* region.

In a pin diode with a concentration of impurities in the *p* and *n* regions at 10^{18} cm^{-3}, and $t_{n^-} = 100$ μm, this situation appears under operating conditions in which 10 kA/cm^2 @ $V_F = 3$ V. The dashed line in Fig. 10 shows the electric field distribution (approximately 200 V/cm in the flat area) at this point. Incidentally, the gray line represents the electric field distribution (approximately 800 V/cm in the flat area) for 100 kA/cm^2 @ $V_F = 10$ V).

At 10 kA/cm^2 @ $V_F = 3$ V, the extreme peak in the built-in electric field at each junction boundary disappears, and the difference in the electrostatic potential (ψ) is very small. As a result, the potential distribution in the diode, including the *p* and *n* regions, is virtually linear.*

Under these conditions, an approximation in which "the net current density (J_h, J_e) is effectively zero" as described in Section 4 clearly does not hold. As a result, an approximation of the carrier density (n_e, n_h) using the Boltzmann distribution cannot be expected to hold. However, the carrier density product ($n_e n_h$) in the junction provides an almost constant value, as shown in Table 2.†

*The changes at the junction boundary in the carrier density become very small. Moreover, when V_F is over 10 V, the ratio of the hole current to the electron current is much larger. As a result, the carrier density in the n^- region is raised significantly near the anode side.

†At $V_F = 3$ V, about 1.3 times greater; at $V_F = 30$ V, about 1.6 times greater or less.

Table 2. $n_e n_h$ values for near junctions in large-current operations (n, p-region: 10^{18} cm^{-3}, 10 μm)

V_F	$Sim.J_F$	Cathode n	K.side n^-	A.side n^-	Anode p
3 V	16.5	0.74	0.87	0.71	0.59
10 V	144	4.9	6.2	3.8	2.8
30 V	1,120	9.2	12	6.1	3.8
(unit)	kA/cm^2	10^{36} cm^{-3}	10^{36}cm^{-3}	10^{36}cm^{-3}	10^{36}cm^{-3}

The results in Table 2, obtained by the simulator using the simultaneous inequalities in Eqs. (24) through (28), can be explained in terms of physics as shown below. The law of mass action* [$n_{e1}n_{e2}/n_{e2}n_{h2} = K(T)$], in which the ratio of the products of the two reactive particle densities on both sides of the boundary are constant (function of temperature), is a highly general law [8] which holds without presupposing a Boltzmann distribution. The equilibrium constant $K(T)$ becomes $K(T) = 1$ per Eqs. (34) and (35) when the Boltzmann distribution (under small-current operation) can be applied [in other words, $n^2 = (N + \Delta n)\Delta n$]. The reason the Boltzmann factor (kT) does not appear clearly in $K(T)$ is that the coefficients for the free electrons and the holes are inverses of each other.† The function in which the product ($n_e n_h$) of the free electron and hole densities is constant can be expected to take the form of a distribution, and as a result $n^2 \approx (N + \Delta n)\Delta n$ is reasonable for the large-current operation.

7. Carrier Distribution When Recombination Occurs

When there is no carrier recombination in the small- or medium-current operations ($V_F \le 1$ V), the carrier distribution in the i region is basically linear (Fig. 7). When there is carrier recombination, the holes (n_h) decrease from the p anode to the n cathode, and instead the free electron density (n_e) rises.‡ For this reason, on the p anode side in the i region, there is a surplus positive charge as $n_h(x) + N_I > n_e(x)$, and on the n cathode side there is a surplus negative charge where $n_h(x) + N_I < n_e(x)$. As a result of these surplus charges, a peaking electric field (from the anode to the cathode) occurs§ in the i region, as shown by the solid line in Fig. 10. The division voltage (V_k and V_a) at the cathode junction and the anode junction decreases by the amount that the division voltage (V_d) in the i region increases, that is, the integral amount of the electric field in it (refer to Fig. 1). Then the densities (n_e, n_h) of the free electrons and the hole electrons also decrease at both edges of the i region. As a result, the amount of surplus charge on both sides of the i region decreases. The strength of the electric field weakens, and the division voltage (V_d) also drops. The distributions [$n_e(x)$, $n_h(x)$] of the charge density in the i region and the division voltage (V_d) are determined by this balance. Ultimately, if there is a recombination mechanism present, then the carrier distribution in the pin diode takes the shape of a bowl.

8. General Evaluation of the On Voltage during Large-Current Operation

On both edges of the i region, the function in which the drift current in the i region and the diffusion current in the p or n region are (almost) equal holds in general [Eq. (46)]. For instance, if n represents the carrier concentration ($n_{eK} = n_{hK}$) on the i side of the junction boundary on the cathode side and Δn represents the hole density (n_{hn}) on the n side, then the free electron density (n_{en}) in the same position is the sum of the n-type impurity concentration ($N = N_n$) and Δn such that the charge neutrality condition is satisfied. As was described in Section 6, the relationship [$n^2 \approx (N + \Delta n)\Delta n$] can be expected to hold between these carrier densities. If Δn found in Eq. (46) is substituted for Δn in this relationship, then the approximate equation in Eq. (47) results.* If each side of Eq. (47) is divided by N, and the resulting Δn is substituted into the third part of Eq. (46) again, then Eq. (48) results. These relational equations can be broadly applied whether or not recombination is present, if the difference ($n_e - n_h \approx N_I$) between n_e and n_h in the i region can be ignored in the operating region. However, the electric field strength (E_0) in Eq. (48) is the value at the edge of the i region.

$$J \approx 2qn\mu_I E \approx 2\mu kT\frac{\Delta n}{\Delta x} \tag{46}$$

$$n^2 \approx (N + \Delta n)\Delta n \approx N\Delta n \approx N\frac{qnE\Delta x}{kT} \tag{47}$$

$$J \approx 2qn\mu E_0 \approx 2\frac{q^2\mu}{kT}E_0{}^2 N\Delta x \tag{48}$$

n and μ_I represent the carrier density ($\approx n_e \approx n_h$) and the mobility on the i region side. N, μ, and Δx are the concentration of impurities, the mobility, and the thickness in the

*Equations (34), (35), (44), and (45) in Section 5 are also a representation of the law of mass action.

†For instance, if $n_e \propto \exp^{-A}$, then $n_h \propto \exp^{A}$.

‡The carrier density distribution (n_e, n_h) for the n and p regions does not change. Over a lifetime, the diffusion coefficient (D) and the mobility (μ) are not directly affected. As a result, if the thickness (t_p, t_n) of the n and p regions, and the operating current density (J_e, J_h) can be determined, then n_e and n_h are determined based on Eqs. (2) and (3).

§In small-current operation (solid line), the positive side is on the order of dozens of volts per centimeter, and the negative side is on the order of several thousand kilovolts per centimeter.

*The difference in the mobility of the hole electrons and the free electrons, and the difference in the mobility in the i region or in the p or n region are ignored.

Table 3. Comparison between Eq. (48) and simulator

V_F	$Calc.J_F$	$Simu.J_F$	ratio	μ	$actualE_0$
3 V	16.5	7.9	x 2.1	150	200
10 V	144	66	x 2.3	120	800
30 V	1,120	217	x 5.1	100	2,400
(unit)	kA/cm^2	kA/cm^2	–	cm^2/Vs	V/cm

p or *n* region. The electric field strength (E_0) on the edge of the *i* region can be approximated with the average electric field of the device overall.*

Table 3 gives a comparison of the simulator output values (not including band gap narrowing or carrier recombination) and the results of calculations using Eq. (48). The mobility in the *p* or *n* region obtained in the simulator is used as μ in Eq. (48) [if the simulation value (μ_l) in the n^- region is used, the error is larger). Because of a fivefold error at most even at $V_F = 30$ V with current at 200 kA/cm^2 flowing, Eq. (48) is deemed valid for up to several dozen kiloamperes per square centimeter. The error in $V_F = 3$ V (≈ 10 kA/cm^2 operation) would be a result of the real electric field strength (E_0) in the junction being smaller than the average electric field strength ($\approx V_F/t_{device}$).

Equation (48) shows a propensity for the canonical operating current (*J*) in a pin diode with a long *i* region to be proportional to the product of the thickness (Δ*x*), concentration (*N*) of impurities in the anode *p* region and the cathode *n* region, and the square of the (average) electric field strength (E_{ave}) in the *i* region. The dependence on the thickness (Δ*x*) and the concentration (*N*) of impurities is confirmed by using characteristics such as the on voltage and inverse recovery time (in other words, the cumulative carrier density when on) of the transparent-type pin diode with a structure similar to the diode in question here.

The term transparent stems from a low concentration of impurities, along with the *p* region and *n* region being thin at less than 2 to 3 μm, and as a result, the carrier passing through these regions with virtually no attenuation. A diode with this configuration tends to have a short inverse recovery time even if its lifetime is long.

Equation (48) is a rough model that presupposes a symmetrical configuration for the *p* region and *n* region, that must use the mobility (μ) obtained by the simulation, and that does not take into consideration the lifetime contributions or the effects of band gap narrowing. However, the mobility (μ) in the *p* or *n* region with high concentrations does not much depend on the operating current density. As a result, it is a rough measure when lifetime control is not performed in a power device (diode, GTO, or IGBT) with a basic pin configuration.

For instance, if $N \approx 10^{18}$ cm^{-3}, $\Delta x \approx 1$ μm, and $\mu \approx$ 100 cm^2/Vs, then the on voltage when 1 kA/cm^2 is flowing through a 1-mm-length pin device (equivalent to 10-kV-resistance thyristor or IGBT on silicon) without lifetime control should be about 14 V.

*On both edges of the *i* region where only the drift current is flowing, the carrier densities (n_e, n_h) increase even over a (long) lifetime for default values in the simulator, and so the electric field strength tends to decrease. However, the drop in the mobility (μ) caused by the increase in n_e and n_h suppresses the tendency for the electric field strength to decrease.

9. Good pin Configuration for a Power Device

If the thickness of the *p* region and *n* region with a diode configuration used for the analysis here is further reduced, then a transparent configuration common in recent years as a high-speed diode for an IGBT module results. In the past 10 years this has been shown to be a method that can achieve the ideal of a pin configuration power device in which "the lifetime is lengthened, the concentration of impurities in the *p* region and *n* region is reduced, and the thickness is decreased all at the same time, and as a result the carrier distribution should be lower and flatter" [9]. The author believes that Fig. 1 can be taken as a simple, inexpensive representation, and that this basic structure itself is the best representation of the principles of diode operation.

10. Conclusion

The author attempted a simple explanation of the operating mechanisms found in a pin diode configuration consisting of a minimum number of elements. The following results were obtained.

(1) The basic equation [Eq. (21)] for the low-current operation in a pin diode with a *p* region and an *n* region with low thickness can be derived based on the diffusion current of the minority carriers in the *p* region and the *n* region, and the Boltzmann distribution. Using this idea the author confirmed that carrier recombination is not necessarily a required factor for pin diode operation.

(2) The carrier density product ($n_h n_e$) was reconfirmed as fundamentally constant on both sides of the junction.* However, at the boundary with a region in which band gap narrowing (ΔE_g) occurs due to a high concentration of impurities, a difference of $\exp(-\Delta E_g/kT)$ occurs [Eqs. (44) and (45)]. (This relationship is valid regardless of whether or not carrier recombination occurs.)

(3) It is known experimentally that the pin diode operating current is inversely proportional to the concentration of impurities in the anode as well as the cathode regions at low current densities, and conversely tends to be propor-

*Equation (4) in Ref. 3 is derived by using this relationship.

tional to the thickness and the concentration of impurities in these regions at high current densities. As basic equations that explain the characteristics above, the author was able to obtain Eq. (48) for large-current operation and Eq. (21) for small-current operation.

The analysis here does not include carrier recombination, and as a result has little practical significance. However, the author believes that the simplicity of the results shows the essential characteristics of diode operation. At the very least, the results should be useful for creating flat images of diode operation. In particular, in the analysis of bipolar devices, knowing the internal carrier distribution is important, and as a result item (2) above should be useful.

REFERENCES

1. Takahashi K. Semiconductor engineering, 2nd ed. Morikita Publishing; 1993. Section 5.2. (in Japanese)
2. Takata I. Small current operation model of pin diodes. 2005 IEEJ annual meeting proceeding, 4-008, p 11–12. (in Japanese)
3. Naito M, Matsuzaki H, Ogawa T. High current characteristics of asymmetrical p-i-n diodes having low forward voltage drops. IEEE Trans ED 1976;23:945–949.
4. Institute of Electrical Engineers of Japan (editor). Power device and power IC handbook. Corona Publishing; 1996. (in Japanese)
5. Seeger K. Semiconductor physics, 4th ed. Springer-Verlag; 1989. p 109.
6. Kurata M. Numerical analysis for semiconductor. Lexington Books; 1982. Section 2.6.
7. van der Ziel A. Boundary conditions for forward biased p-n junctions. Solid-State Electron 1973;16: 1509–1511.
8. Fermi E. Thermodynamics. Prentice-Hall; 1937. Chapters 6 and 7.
9. Takata I. The leading edge of IGBT. Institute of Electrical Engineering of Japan; 1996. p 17–25. (in Japanese)

AUTHOR

Ikunori Takata (member) completed a master's in the Department of Science and Research at Kobe University in 1974 and joined Mitsubishi Electric Corp. He has been pursuing the manufacture and development of semiconductor power electronics for transistor modules and high-speed diodes. He has intended to explain semiconductors without using quantum mechanics. In particular, he is interested in breakdown phenomenon under strong electric fields, and at present he is working with the Power Electronic Department at the Advanced Technology R&D Center.